Sustainable Energy & Fuels

Assessing the True Power of Bifacial Perovskite Solar Cells under Concurrent Bifacial Illumination

Journal:	*Sustainable Energy & Fuels*
Manuscript ID	SE-COM-03-2021-000314.R1
Article Type:	Communication
Date Submitted by the Author:	24-Apr-2021
Complete List of Authors:	Song, Zhaoning; University of Toledo, Physics and Astronomy Chen, Cong; University of Toledo, Physics and Astronomy Li, Chongwen; University of Toledo, Physics and Astronomy Rijal, Suman; University of Toledo, Physics and Astronomy Chen, Lei; University of Toledo, Physics and Astronomy Li, You; University of Toledo, Physics and Astronomy Yan, Yanfa; University of Toledo, Physics and Astronomy

Assessing the True Power of Bifacial Perovskite Solar Cells under Concurrent Bifacial Illumination

Zhaoning Song, Cong Chen, Chongwen Li, Suman Rijal, Lei Chen, You Li, and Yanfa Yan**

Department of Physics and Astronomy and Wright Center for Photovoltaics Innovation and Commercialization, The University of Toledo, Toledo, Ohio 43606, United States

AUTHOR INFORMATION

Corresponding Author

*zhaoning.song@utoledo.edu and yanfa.yan@utoledo.edu

ABSTRACT

An accurate assessment of bifacial solar cells under concurrent bifacial illumination is critical to evaluate their real photovoltaic performance. In this work, we demonstrate bifacial perovskite solar cells with bifacial equivalent power conversion efficiencies of 21% and 26% under concurrent bifacial illumination with an albedo of 0.2 and 0.5, respectively. A detailed balance efficiency limit analysis further reveals the full potential of bifacial perovskite solar cells.

Introduction

Metal halide perovskite solar cells (PSCs) have gained significant interest in the past decade due to their rapidly increasing power conversion efficiency (PCE) to more than 25%,[1] ease of production using low-temperature solution-based processes,[2-4] and projected low manufacturing costs.[5] With the overwhelming success in the premature stage, considerable research effort has now been directed toward moving this emerging photovoltaic (PV) technology from lab to market.[6] In this regard, it is essential to achieve a low dollar per watt ($/W) perovskite module cost that can compete with the low price (<US$0.4/W)[7] of today's mainstream crystalline silicon solar panels. Such a low module cost requires PSCs to deliver high output powers at relatively low production costs. To achieve this goal, many strategies have been proposed for enhancing the power generation of PSCs, such as tandem,[8-11] concentrated,[12, 13] bifacial solar cells,[14-18] or their combinations.[19, 20] Among them, bifacial solar cells are particularly promising for practical use because they can boost the power output of solar models without a significant increase in the production costs associated with additional subcells for

tandems or the balance of systems for concentrated PV. For practical applications, bifacial PV modules can be installed using vertical mounting or with a high albedo surface (reflector).[21-23]

Rather than cover the entire back surface of a solar cell with an opaque metal electrode, bifacial solar cell designs employ a transparent conducting electrode (often combined with finger grids) to enable light-harvesting from both front and rear sides, allowing the device to collect albedo light from the ground. Bifacial solar modules with a power boost of an overall efficiency of more than 10% are top trending products by silicon solar manufacturers in today's PV market.[24] However, efficient bifacial designs have rarely been realized in inorganic thin-film solar cells, such as cadmium telluride and copper indium gallium selenide, mainly due to the absence of a built-in electric field near the rear surface of thin-film absorbers and insufficient lifetime and diffusion length that sustain the transport of photoexcited minority carriers generated at the rear side to the front heterojunction.[25, 26]

Unlike conventional thin-film PV, PSCs provide a unique opportunity to leverage their bifacial potential because of their outstanding optoelectrical properties (e.g., high absorption coefficients, long carrier lifetimes, defect tolerance, etc.) and device architectures that do not rely on p-n junctions. To date, there are many reports on near-infrared (NIR) transparent PSCs with an emphasis on the semi-transparent solar cells for four-terminal tandem devices[27-29] and building-integrated photovoltaics (BIPV),[30] but their practical application as bifacial devices are currently underperformed and undervalued (Table S1). Most of the bifacial PSC studies only measured device performance under single-side illumination conditions and calculated the bifaciality, i.e., the efficiency ratio when illuminated from the front and rear side.[17] The PV performance of bifacial PSCs under concurrent bifacial illumination or adjustable albedo light has not been accurately tested and reported. Particularly, the impact of a higher illumination intensity on the PV parameters of bifacial PSCs has yet to be determined. The perovskite PV community has not yet adopted the test standard (IEC TS 60904-1-2, Measurement of current-voltage characteristics of bifacial PV device) that has been proposed for commercial bifacial Si solar cells.[31]

To fulfill the need for accurately assessing the PV performance of bifacial PSCs, in this work, we combine experimental and theoretical analyses to evaluate the practical potential of bifacial PSCs. We show that the bifacial PSCs deliver output power densities of ~210 and 260 W/m^2 with an albedo of 0.2 and 0.5, respectively. We further perform theoretical analysis to show the relationship between the maximum output power density and albedo light intensity of an arbitrary bifacial solar cell, highlighting the full potential of bifacial PSCs.

Results and discussion

To demonstrate bifacial applications, we fabricated PSCs with a bifacial device architecture of MgF_2/glass/ITO/poly(triarylamine) (PTAA)/perovskite/C_{60}/SnO_2/ITO/Ag grid/MgF_2, as shown in **Figure 1a**. We selected a methylammonium (MA)-free formamidinium (FA)-based perovskite absorber with a composition of $FA_{0.8}Cs_{0.2}Pb(I_{0.9}Br_{0.1})_3$ because of its better thermal and photostability than MA-contained perovskite absorbers.[32] Additionally, the so-called p-i-n device configuration is chosen because it shows decent PV performance with negligible current density-voltage

(J-V hysteresis).[33] Detailed fabrication procedures are provided in the Electronic Supplementary Information (ESI). **Figure 1b** shows the J-V plots of a typical device under single-side illumination. Under the glass (film) side illumination, the cell delivers a PCE of 18.4 (17.5)%, with a V_{OC} of 1.124 (1.119)V, a J_{SC} of 20.4 (19.5) mA/cm^2, and a FF of 80.2 (80.1)%. The PCE of our semi-transparent PSCs are in a good level in comparison to state-of-the-art devices (Table S1). External quantum efficiency (EQE) measurement (**Figure 1c**) reveals that the slightly lower J_{SC} under the film-side illumination is ascribed to the lower conversion efficiencies below 500 nm. EQE simulation (Figure S1) was performed using optical properties obtained by spectroscopic ellipsometry, following our previously reported method.[34] The result shows that the optical loss at short wavelengths is mainly attributed to the parasitic absorption of the ITO and C_{60} layer. There is also room for the optimization of the film stack thickness and anti-reflection coatings of PSCs, which can further enhance the J_{SC} and PCE of the bifacial device. This bifacial PSC exhibits steady-state efficiencies of 18.3% and 17.5% when illuminated from the glass and film side, respectively (**Figure 1d**), consistent with the PCEs determined by the J-V measurements. The bifaciality of this device, which is defined as the PCE ratio under the front and rear illumination, is thus determined to be 0.96, revealing the efficient utilization of photons incident from both sides of the device. With proper tuning of the device structure, the J_{SC} difference in bifacial PSCs can be adjusted to almost zero, and a bifaciality of 1 can be achieved.[35]

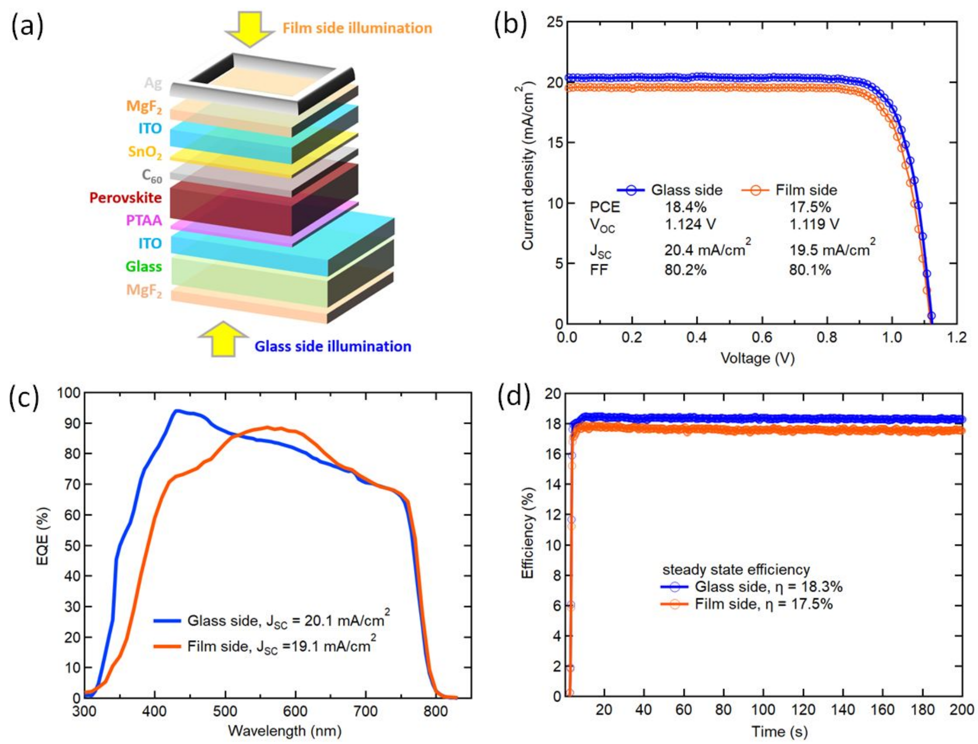

Figure 1. (a) Schematic device structure of a bifacial perovskite solar cell. (b) J-V, (c) EQE, and (d) steady-state efficiency curves of a typical bifacial perovskite solar cell under single (glass or film) side illumination.

To accurately evaluate the PV performance of bifacial PSCs, we built a setup to measure the J-V characteristics of bifacial devices under concurrent bifacial illumination (Figure S2). **Figure 2a** shows the J-V curves of a bifacial PSC under different bifacial illumination conditions, consisting of a standard AM1.5G front illumination and an adjustable rear-side illumination to simulate albedo light. The J_{SC} and V_{OC} of the device increases while FF slightly decreases with increasing albedo light intensity (**Figure 2b-d**), leading to a higher output power density under high albedo illumination (**Figure 2e**). The increased V_{OC} is attributed to a higher photocurrent density because the V_{OC} of a solar cell is proportional to Ln(J_{SC}/J_0+1), where J_{SC} and J_0 are the photogenerated and dark saturation current densities, respectively.[36] The decreased FF is mainly due to the thermal loss at the series resistance caused by the relatively high resistance value of two ITO electrodes.[37] A figure of merit named bifacial equivalent efficiency,[15] representing the efficiency of a monofacial solar cell needed to generate the same power density under the same operating condition, is then used to characterize the device. **Figure 2e** shows that the PSC achieves a bifacial equivalent efficiency of up to 26% under an albedo of 0.5. Note that an albedo of ~0.5 is feasible with a high reflective arrangement[38] or a high albedo surface, such as a white fiberglass rooftop (Figure S3).[39]

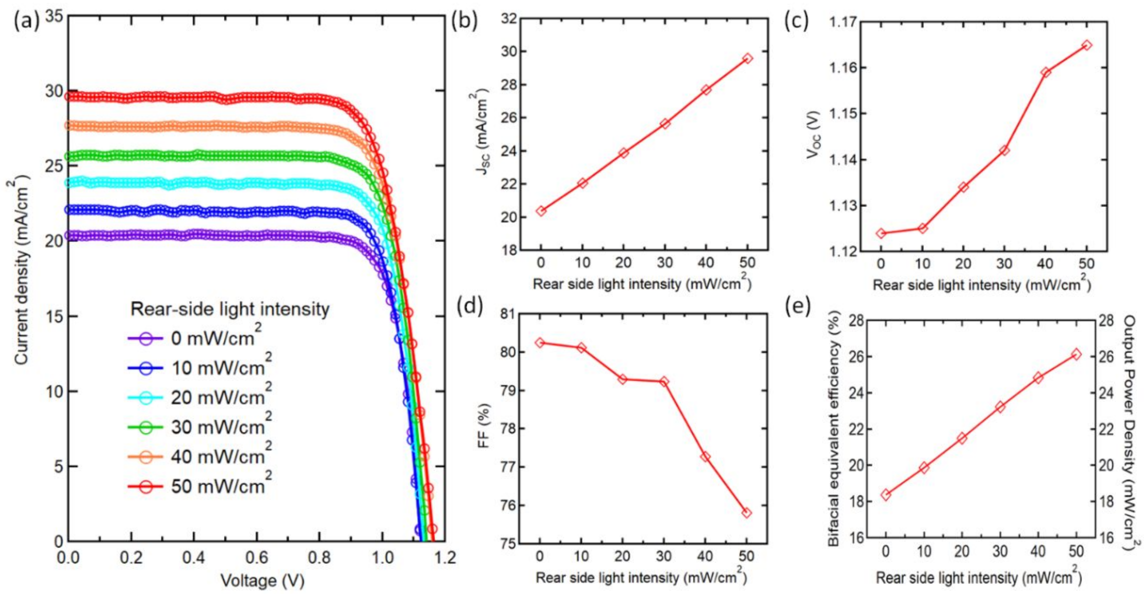

Figure 2. (a) J-V curves of the device under concurrent bifacial illumination with various light intensities (0 to 50 mW/cm^2) from the rear (film) side. (b) J_{SC}, (c) V_{OC}, FF, and (e) bifacial equivalent efficiency and output power density of the device under different concurrent bifacial illumination conditions.

For more practical applications with relatively low albedo surfaces, the proposed bifacial PV test standard uses an albedo of ~0.2.[31] To evaluate the potential for real-world applications, we compare the PV performance of bifacial PSCs with opaque PSCs with an average PCE of ~20% (Figure S3). **Figure 3** shows that under the standard testing condition with a back-side illumination intensity of 20 mW/cm^2, bifacial PSCs deliver a higher power output than their monofacial counterparts with an opaque (Ag) back electrode. It is worth noting that typical concrete surfaces or grass ground have albedo higher than 0.2 (Figure S4). Another benefit for bifacial PSCs is better device stability than conventional monofacial cells. Bifacial PSCs eliminate direct contact with metal electrodes and cover the top surface of the film stack with a uniform and impermeable metal oxide coating, which is known to suppress the halide induced electrode corrosion and the egress of volatile species of perovskite absorbers.[40, 41] In agreement with the literature,[42] we found that bifacial PSCs exhibit much-improved stability than monofacial PSCs under thermal and light stresses (Figure S5). The results show that the long-term stability of bifacial PSCs is feasible, provided that the intrinsic stability issue of perovskite absorbers can be addressed. The potential of simultaneously achieving high PCE and stability makes bifacial PSCs promising for practical applications.

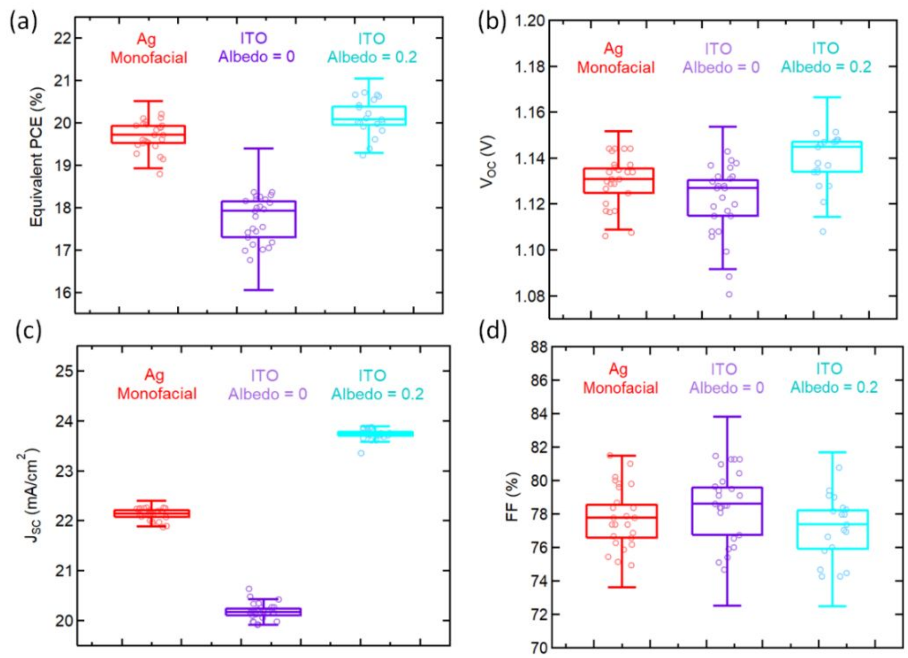

Figure 3. Statistical distributions of (a) equivalent PCE, (b) J_{SC}, (c) V_{OC}, and (d) FF of monofacial PSCs with Ag electrodes and bifacial PSCs with ITO electrodes under two different (Albedo = 0 and 0.2) bifacial illumination conditions.

To further assess the full potential of bifacial PSCs, we analyze the detailed balance bifacial equivalent efficiency limits of bifacial solar cells with different absorber bandgaps by modifying the Shockley–Queisser thermodynamic limit calculation.[43] Various albedo light conditions (**Figure 4a**) were considered the secondary light source to add to the photocurrent generation. Details of the analysis are provided in the ESI. The results show that with a uniform albedo of 0.1 to 0.5, the output power density (or equivalent bifacial efficiency) of bifacial PSCs can be increased by 10.2% to 51.5% for a typical perovskite bandgap range of 1.45 to 1.75 eV (Figure S6). The bifacial illumination with different albedo surfaces can boost the bifacial equivalent efficiency to more than 35-50% or the output power density of 35 to 60 mW/cm^2 (**Figure 4b**). Such increased power generation can reduce the $/W cost of perovskite PV modules by 10 to ~33% based on our previous technoeconomic analysis (Figure S7),[5] which may make bifacial PSCs one of the cheapest PV technologies in the future.

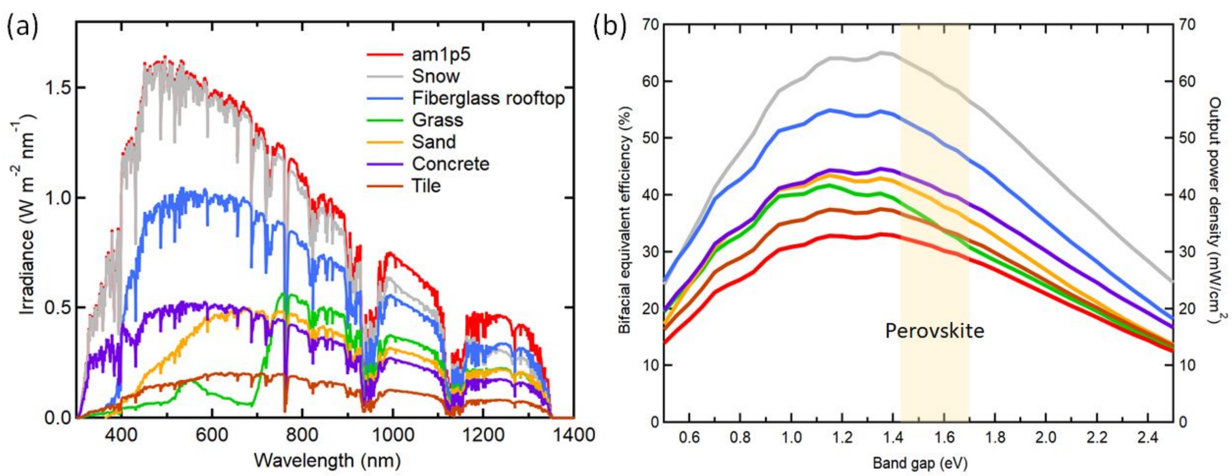

Figure 4. (a) Albedo spectra of different ground materials under AM1.5 solar illumination, including snow, fiberglass rooftop, grass, yellow sand, concrete, and tile. The reflectance data is adapted from NASA's ECOSTRESS Spectral Library. (b) Detailed balance bifacial equivalent efficiency and output power density limit of bifacial solar cells with different absorber bandgaps with different albedo surfaces. The shaded area highlights the bandgap range for high-efficiency PSCs.

Conclusion

In sum, we demonstrated that bifacial PSCs have the potential to achieve a higher output power density than monofacial devices under a proper albedo light illumination and exhibit enhanced device stability. Theoretical analysis shows the bifacial solar cells are promising to convert more solar energy into electricity with a high albedo surface. Overall, bifacial designs, therefore, deserve serious consideration for the future commercialization of perovskite PV.

Conflicts of interest

The authors declare no competing financial interest.

Author contribution

Z. S. and Y. Y. conceived the project. Z. S. carried out the device fabrication, measurements, and theoretical calculation. C. C., C. L., and S. R. help with the device fabrication. L. C. and Y. L. help with the characterization and stability measurement. All the authors discussed the results and commented on the manuscript. Z. S. and Y. Y. supervised the project.

Acknowledgements

This material is based upon work supported by the U.S. Department of Energy's Office of Energy Efficiency and Renewable Energy (EERE) under the Solar Energy Technologies Office Award Numbers DE-EE0008753 and DE-EE0008790, and by the U.S. Air Force Research Laboratory under agreement number FA9453–19-C-1002. The U.S. Government is authorized to reproduce and distribute reprints for Governmental purposes notwithstanding any copyright notation thereon. Disclaimer: The views and conclusions contained herein are those of the authors and should not be interpreted as necessarily representing the official policies or endorsements, either expressed or implied, of the U.S. Air Force Research Laboratory or the U.S. Government.

References

1. J. J. Yoo, G. Seo, M. R. Chua, T. G. Park, Y. Lu, F. Rotermund, Y.-K. Kim, C. S. Moon, N. J. Jeon, J.-P. Correa-Baena, V. Bulović, S. S. Shin, M. G. Bawendi and J. Seo, *Nature*, 2021, **590**, 587-593.
2. Y. Y. Kim, T.-Y. Yang, R. Suhonen, A. Kemppainen, K. Hwang, N. J. Jeon and J. Seo, *Nat. Commun.*, 2020, **11**, 5146.
3. D. Burkitt, R. Patidar, P. Greenwood, K. Hooper, J. McGettrick, S. Dimitrov, M. Colombo, V. Stoichkov, D. Richards, D. Beynon, M. Davies and T. Watson, *Sustainable Energy Fuels*, 2020, **4**, 3340-3351.
4. D. Angmo, G. DeLuca, A. D. Scully, A. S. R. Chesman, A. Seeber, C. Zuo, D. Vak, U. Bach and M. Gao, *Cell Reports Physical Science*, 2021, **2**, 100293.
5. Z. Song, C. L. McElvany, A. B. Phillips, I. Celik, P. W. Krantz, S. C. Watthage, G. K. Liyanage, D. Apul and M. J. Heben, *Energy Environ. Sci.*, 2017, **10**, 1297-1305.
6. A. Extance, *Nature*, 2019, **570**, 429-432.
7. PV Insights, http://pvinsights.com/, (accessed 15 January 2021).
8. Z. Song, C. Chen, C. Li, R. A. Awni, D. Zhao and Y. Yan, *Semicond. Sci. Technol.*, 2019, **34**, 093001.
9. Y. Hou, E. Aydin, M. De Bastiani, C. Xiao, F. H. Isikgor, D.-J. Xue, B. Chen, H. Chen, B. Bahrami, A. H. Chowdhury, A. Johnston, S.-W. Baek, Z. Huang, M. Wei, Y. Dong, J. Troughton, R. Jalmood, A. J. Mirabelli, T. G. Allen, E. Van Kerschaver, M. I. Saidaminov, D. Baran, Q. Qiao, K. Zhu, S. De Wolf and E. H. Sargent, *Science*, 2020, **367**, 1135-1140.
10. C. Li, Z. Song, C. Chen, C. Xiao, B. Subedi, S. P. Harvey, N. Shrestha, K. K. Subedi, L. Chen, D. Liu, Y. Li, Y.-W. Kim, C.-s. Jiang, M. J. Heben, D. Zhao, R. J. Ellingson, N. J. Podraza, M. Al-Jassim and Y. Yan, *Nat. Energy*, 2020, **5**, 768-776.

11. A. Al-Ashouri, E. Köhnen, B. Li, A. Magomedov, H. Hempel, P. Caprioglio, J. A. Márquez, A. B. Morales Vilches, E. Kasparavicius, J. A. Smith, N. Phung, D. Menzel, M. Grischek, L. Kegelmann, D. Skroblin, C. Gollwitzer, T. Malinauskas, M. Jošt, G. Matič, B. Rech, R. Schlatmann, M. Topič, L. Korte, A. Abate, B. Stannowski, D. Neher, M. Stolterfoht, T. Unold, V. Getautis and S. Albrecht, *Science*, 2020, **370**, 1300-1309.
12. H. Baig, H. Kanda, A. M. Asiri, M. K. Nazeeruddin and T. Mallick, *Sustainable Energy Fuels*, 2020, **4**, 528-537.
13. Q. Lin, Z. Wang, H. J. Snaith, M. B. Johnston and L. M. Herz, *Adv. Sci.*, 2018, **5**, 1700792.
14. F. Fu, T. Feurer, T. Jager, E. Avancini, B. Bissig, S. Yoon, S. Buecheler and A. N. Tiwari, *Nat Commun*, 2015, **6**, 8932.
15. H. Wang, H. A. Dewi, T. M. Koh, A. Bruno, S. Mhaisalkar and N. Mathews, *ACS Appl. Energy Mater.*, 2020, **12**, 484-493.
16. R. A. Jagt, T. N. Huq, S. A. Hill, M. Thway, T. Liu, M. Napari, B. Roose, K. Gałkowski, W. Li, S. F. Lin, S. D. Stranks, J. L. MacManus-Driscoll and R. L. Z. Hoye, *ACS Energy Lett.*, 2020, **5**, 2456-2465.
17. T. Li, W. A. Dunlap-Shohl and D. B. Mitzi, *ACS Appl. Energy Mater.*, 2020, **3**, 9493-9497.
18. A. J. Bett, K. M. Winkler, M. Bivour, L. Cojocaru, Ö. Ș. Kabakli, P. S. C. Schulze, G. Siefer, L. Tutsch, M. Hermle, S. W. Glunz and J. C. Goldschmidt, *ACS Appl. Energy Mater.*, 2019, **11**, 45796-45804.
19. M. De Bastiani, A. J. Mirabelli, Y. Hou, F. Gota, E. Aydin, T. G. Allen, J. Troughton, A. S. Subbiah, F. H. Isikgor, J. Liu, L. Xu, B. Chen, E. Van Kerschaver, D. Baran, B. Fraboni, M. F. Salvador, U. W. Paetzold, E. H. Sargent and S. De Wolf, *Nat. Energy*, 2021, **6**, 167-175.
20. R. H. Ahangharnejhad, W. Becker, J. Jones, A. Anctil, Z. Song, A. Phillips, M. J. Heben and I. Celik, *Cell Reports Physical Science*, 2021, **2**, 100344.
21. M. R. Khan, A. Hanna, X. Sun and M. A. Alam, *Applied Energy*, 2017, **206**, 240-248.

22. T. Baumann, H. Nussbaumer, M. Klenk, A. Dreisiebner, F. Carigiet and F. Baumgartner, *Solar Energy*, 2019, **190**, 139-146.
23. X. Sun, M. R. Khan, C. Deline and M. A. Alam, *Applied Energy*, 2018, **212**, 1601-1610.
24. R. Guerrero-Lemus, R. Vega, T. Kim, A. Kimm and L. E. Shephard, *Renewable Sustainable Energy Rev.*, 2016, **60**, 1533-1549.
25. A. B. Phillips, K. K. Subedi, G. K. Liyanage, F. K. Alfadhili, R. J. Ellingson and M. J. Heben, *ACS Applied Energy Materials*, 2020, **3**, 6072-6078.
26. K. K. Subedi, A. B. Phillips, N. Shrestha, F. K. Alfadhili, A. Osella, I. Subedi, R. A. Awni, E. Bastola, Z. Song, D.-B. Li, R. W. Collins, Y. Yan, N. J. Podraza, M. J. Heben and R. J. Ellingson, *Nano Energy*, 2021, **83**, 105827.
27. R. K. Kothandaraman, Y. Jiang, T. Feurer, A. N. Tiwari and F. Fu, *Small Methods*, 2020, **4**, 2000395.
28. Z. Ying, Y. Zhu, X. Feng, J. Xiu, R. Zhang, X. Ma, Y. Deng, H. Pan and Z. He, *Adv. Mater. Interfaces*, 2021, **8**, 2001604.
29. Z. Ying, X. Yang, J. Zheng, Y. Zhu, J. Xiu, W. Chen, C. Shou, J. Sheng, Y. Zeng, B. Yan, H. Pan, J. Ye and Z. He, *J. Mater. Chem. A*, 2021, DOI: 10.1039/D1TA01180D.
30. S.-H. Lim, H.-J. Seok, M.-J. Kwak, D.-H. Choi, S.-K. Kim, D.-H. Kim and H.-K. Kim, *Nano Energy*, 2021, **82**, 105703.
31. T. S. Liang, M. Pravettoni, C. Deline, J. S. Stein, R. Kopecek, J. P. Singh, W. Luo, Y. Wang, A. G. Aberle and Y. S. Khoo, *Energy Environ. Sci.*, 2019, **12**, 116-148.
32. Z. Song, C. Wang, A. B. Phillips, C. R. Grice, D. Zhao, Y. Yu, C. Chen, C. Li, X. Yin, R. Ellingson, M. Heben and Y. Yan, *Sustainable Energy & Fuels*, 2018, **2**, 2460-2467.
33. C. Chen, Z. Song, C. Xiao, R. A. Awni, C. Yao, N. Shrestha, C. Li, S. S. Bista, Y. Zhang, L. Chen, R. J. Ellingson, C.-S. Jiang, M. Al-Jassim, G. Fang and Y. Yan, *ACS Energy Lett.*, 2020, **5**, 2560-2568.
34. B. Subedi, Z. Song, C. Chen, C. Li, K. Ghimire, M. M. Junda, I. Subedi, Y. Yan and N. J. Podraza, *ACS Appl. Energy Mater.*, 2021, **13**, 4923-4934.

35. F. Fu, T. Feurer, T. P. Weiss, S. Pisoni, E. Avancini, C. Andres, S. Buecheler and A. N. Tiwari, *Nat. Energy*, 2016, **2**, 16190.
36. C. Li, Z. Song, D. Zhao, C. Xiao, B. Subedi, N. Shrestha, M. M. Junda, C. Wang, C.-S. Jiang, M. Al-Jassim, R. J. Ellingson, N. J. Podraza, K. Zhu and Y. Yan, *Adv. Energy Mater.*, 2019, **9**, 1803135.
37. D. Kiermasch, L. Gil-Escrig, H. J. Bolink and K. Tvingstedt, *Joule*, 2019, **3**, 16-26.
38. A. Cuevas, A. Luque, J. Eguren and J. del Alamo, *Solar Energy*, 1982, **29**, 419-420.
39. A. M. Baldridge, S. J. Hook, C. I. Grove and G. Rivera, *Remote Sensing of Environment*, 2009, **113**, 711-715.
40. K. A. Bush, C. D. Bailie, Y. Chen, A. R. Bowring, W. Wang, W. Ma, T. Leijtens, F. Moghadam and M. D. McGehee, *Adv. Mater.*, 2016, **28**, 3937-3943.
41. R. Cheacharoen, C. C. Boyd, G. F. Burkhard, T. Leijtens, J. A. Raiford, K. A. Bush, S. F. Bent and M. D. McGehee, *Sustainable Energy Fuels*, 2018, **2**, 2398-2406.
42. C. C. Boyd, R. Cheacharoen, K. A. Bush, R. Prasanna, T. Leijtens and M. D. McGehee, *ACS Energy Lett.*, 2018, **3**, 1772-1778.
43. W. Shockley and H. J. Queisser, *Journal of Applied Physics*, 1961, **32**, 510-519.